Planetary Defense Conference 2013
Flagstaff, AZ, USA
IAA-PDC13-04-24

Uncertainty Quantification in Impulsive Deflection Scenarios[☆]

Kirsten Howley, Joseph Wasem[*]

Lawrence Livermore National Laboratory, L-031, 7000 East Ave., Livermore, CA

Abstract

For the majority of Near-Earth Object (NEO) impact scenarios, optimal deflection strategies use a massive impactor or a nuclear explosive, either of which produce an impulsive change to the orbit of the object. However, uncertainties regarding the object composition and the efficiency of the deflection event lead to a non-negligible uncertainty in the deflection velocity. Propagating this error through the resulting orbit will create a positional error envelope at the original time of impact. We calculate an analytic evolution for impulsively deflected NEOs and perform a full propagation of errors that is nonlinear in the deflection velocity vector. This provides a fully nonperturbative solution for the changed orbital parameters, as well as the resulting positional error and corresponding residual impact probability.

Keywords: Uncertainty, Impulsive Deflection, Error Propagation

1. Introduction & Background

For scenarios involving Near-Earth Objects (NEOs) that are revealed to be on a collision course with Earth, most occur with little lead time (often several years or less) or with a relatively large object. In situations such as these, most deflection strategies rely on the use of a massive impactor or a nuclear device to provide the necessary change in velocity for an avoided impact. Both of these possibilities provide a sudden impulse to the NEO, where the orbital parameters governing the motion of the object are changed on timescales that are much shorter than orbital evolution timescales. As such, these changes can be approximated to an extremely high degree as being instantaneous, taking an object with an initial set of orbital parameters and moving it to a new set.

Such an event is shown in a greatly exaggerated sense in Fig. 1. Here the object has initial orbital parameters given by a semi-major axis a, and eccentricity e, and a longitude of pericenter

[☆]LLNL-PROC-632276. This work was performed under the auspices of the U.S. Department of Energy by Lawrence Livermore National Laboratory under Contract DE-AC52-07NA27344, and partially funded by the Laboratory Directed Research and Development Program at LLNL under tracking code 12-ERD-005.

[*]Corresponding Author/Presenter

Email addresses: howley1@llnl.gov (Kirsten Howley), wasem2@llnl.gov (Joseph Wasem)

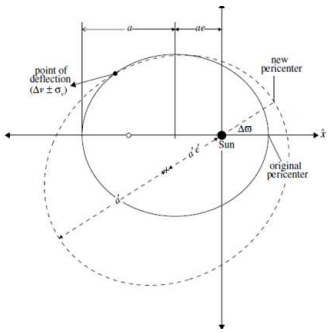

Figure 1: A diagram of the orbital components relevant for the deflection analysis. The original orbit is the solid black line, with the impulsively modified orbit the dashed black line. The original orbital parameters (a and e) as well as the new orbit parameters (a', e', and $\Delta\varpi$) are shown along with the point of deflection. Note that the scenario depicted here involves a much larger Δv than would actually be employed, but has been exaggerated for emphasis.

ϖ (where we have chosen our axes such the $\varpi = 0$ initially). In the limiting case where one neglects all gravitational effects beyond that of the sun one can choose to work purely in a planar geometry. We utilize this approximation here, and note that it is accurate to a very high order in perturbative orbital expansions. The general expression for this orbit in a plane, given the above orbital parameters, is:

$$r = \frac{a(1-e^2)}{1+e\cos(\theta-\varpi)}. \tag{1}$$

Following the deflection event at an arbitrary position on the original orbit, the object will be shifted into a new orbit given by semi-major axis a', eccentricity e', and longitude of perihelion $\varpi' = \Delta\varpi$. This new orbit will be in the same plane as and, critically, will share a common spacetime point with the original orbit: that of the deflection event. Considering the specific angular momentum H and specific energy U of an orbit in terms of the above orbital parameters, one has:

$$H = \sqrt{\mu a(1-e^2)}, \;\; U = -\frac{\mu}{2a}. \tag{2}$$

By calculating the changes to the specific energy and the specific angular momentum during the deflection event, one obtains

$$\begin{aligned}
\Delta H &= H' - H_0 = \vec{r}\times(\vec{v}+\Delta\vec{v}) - \vec{r}\times\vec{v} = \frac{a(1-e^2)}{1+e\cos f_0}\Delta v_\theta \\
\Delta U &= U' - U_0 = \frac{1}{2}(\vec{v}+\Delta\vec{v})^2 - \frac{1}{2}v^2 \\
&= \frac{1}{2}\left(\Delta v_r^2 + \Delta v_\theta^2\right) + \sqrt{\frac{\mu}{a(1-e^2)}}\left(\Delta v_r e\sin f_0 + \Delta v_\theta(1+e\cos f_0)\right)
\end{aligned} \tag{3}$$

for an arbitrary in-plane deflection. Adding the constraint that the new orbit must go through the deflection spacetime point, one can obtain the highly nonlinear relationship between a, e, and ϖ

and a', e', and ϖ':

$$\begin{aligned} a' &= a + \Delta a = a + \frac{\mu \Delta U}{2U(\Delta U + U)} \\ e' &= e + \Delta e = \left(\frac{\left(e^2 - 1\right)(H + \Delta H)^2 \left(U + \Delta U\right)}{H^2 U} + 1 \right)^{1/2} \\ \varpi' &= \Delta \varpi = f_0 - \cos^{-1}\left(\frac{a'(1 - e'^2)}{a(1 - e^2)} \frac{1 + e\cos f_0}{e'} - \frac{1}{e'} \right) \end{aligned} \tag{4}$$

where f_0 is the true longitude at the position of the deflection attempt. Given these relationships between the old orbital parameters and the new one can then switch from working in an angular space parameterized by the true longitude (or true anomaly) to one parameterized by the eccentric anomaly E. This allows the x and y components of the original impact point to be characterized by

$$\begin{pmatrix} x_\oplus \\ y_\oplus \end{pmatrix} = \begin{pmatrix} a(\cos E_\oplus - e) \\ a\sqrt{1 - e^2}\sin E_\oplus \end{pmatrix} \tag{5}$$

with $E_\oplus$ the eccentric anomaly of the impact point. The deflected position of the object at the original impact time can be then determined as

$$\begin{aligned} \begin{pmatrix} x'_\oplus \\ y'_\oplus \end{pmatrix} &= \begin{pmatrix} \cos\varpi' & -\sin\varpi' \\ \sin\varpi' & \cos\varpi' \end{pmatrix} \begin{pmatrix} a'(\cos E'_\oplus - e') \\ a'\sqrt{1 - e'^2}\sin E'_\oplus \end{pmatrix} \\ \Delta r &= \sqrt{(x_\oplus - x'_\oplus)^2 + (y_\oplus - y'_\oplus)^2} \end{aligned} \tag{6}$$

where the relationship between $E_\oplus$ and $E'_\oplus$ can be derived from Eq. 4 in combination with the definitions found in Ref. [1]. It should be noted that the above equations represent the overall steps in the derivation, however many straightforward but important details are being glossed over in the interests of brevity and space.

The final line of Eq. 6 gives the fully nonlinear propagation of an arbitrary deflection velocity $\Delta\vec{v}$ in the plane of the orbit of the NEO, and an extension to the linearized theory given in Ref. [2]. In any realistic deflection attempt there will be multiple sources of possible uncertainty. The complete composition of the object may be poorly understood, including not only elemental composition, but porosity and heterogeneity considerations as well. Indeed, the total mass of the object may not even be known to a high degree of accuracy if only the absolute magnitude of the object has been recorded. Furthermore, the coupling of the deflection attempt with the object will add uncertainty to the final velocity of the deflection. These unknowns will add into a final uncertainty in the deflection velocity delivered to the object, and this error will propagate through the resulting orbit to create a final positional error associated with the mean deflection given in Eq. 6. Finally, uncertainty in the original orbital parameters will also effect the propagation of the velocity error through to the final deflection. All of these factors must be carefully considered in mission planning for a deflection event, and in this proceedings we discuss some specific examples and their final deflection probability distributions.

2. Error Propagation

For the purposes of this proceeding we will assume a Gaussian error in the deflection velocity Δv where the Gaussian distribution is set to zero for values more than 20% above the mean and

renormalized (this stems from the practical belief that while the unknowns in the problem may adversely effect the deflection attempt, they are less likely to cause a significantly greater than expected deflection). Furthermore, to simplify the discussion we will consider only velocity changes with or against the direction of motion of the object, not perpendicular, which are the dominant mode of impulsive deflection at times-to-impact of greater than a few months. The 1σ (i.e. 68% confidence interval) uncertainty level is then expressed simply as

$$\sigma_{\Delta r} \quad = \quad \sigma_{\Delta v} \left| \frac{\partial(\Delta r)}{\partial(\Delta v)} \right|. \tag{7}$$

However, while this simple equation can be determined analytically from the results of Eqns. [1-6], the computation involves a series of chained derivatives and is a very involved calculation. As such it is left as an exercise to the reader. Note that while we have assumed a Gaussian distribution of velocities for the sake of simplicity, this is not strictly necessary.

To evaluate the propagation of errors we choose to examine a fictitious object with the orbital parameters of 2011 AG5 (a = 1.43 and e = 0.39) that has been shifted slightly to impact the Earth on Feb. 4, 2040 (currently its date of closest approach). We call this object 2011 AG5*. In Fig. 2 are plotted the results of a 2 cm/s mean deflection velocity with a 10% error, as a function of time-to-impact (the central black line). Surrounding this is the error envelope created from the propagation of the velocity errors through the equations, where the grey lines moving outward from the nominal deflection are the 1, 2, 3σ bands, respectively.

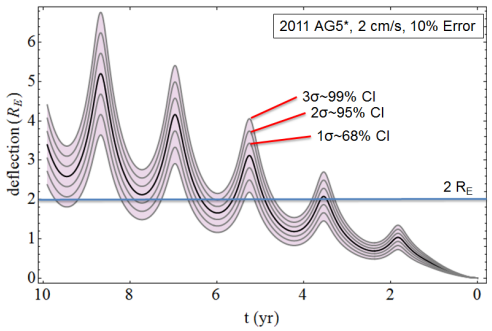

Figure 2: The deflection distance (in Earth radii, R_E) for an object with the orbital parameters of 2011 AG5 as a function of time-to-impact, with associated 1, 2, and 3σ confidence intervals. This curve corresponds to a 2 cm/s mean deflection with a 10% error. The blue horizontal line is a $2R_E$ deflection level, which nominally corresponds to a successful deflection attempt.

One notes immediately that the deflection is more effective at certain points than others. These are the times around when the object is at perihelion, and the error envelope in those time periods is larger as well. At the 3σ level, there is a 99% probability that the actual deflection distance will fall within the outermost grey band. At a time of deflection nearing 10 years this results in a comfortably high chance of mission success, while around 3 years and below it results in a depressing probability of failure. As the community is well aware, the earlier the deflection attempt the greater chance of success it generally has (as a change in velocity in the direction of motion has a greater time over which to work), but with the propagation of the uncertainties through the orbital motion one can be more quantitative about this statement.

3. Confidence Levels

By choosing a deflection distance corresponding to two earth radii (the horizontal blue line in Fig. 2) one can use the Gaussian distribution generated from the propagation of the errors to calculate the probability that the object will be deflected by two earth radii or greater versus the time-to-impact. This results in Fig. 3, which shows the confidence percentage of a successful mission. Note that the resulting confidence levels cluster into several windows near the times of perihelion passage for the object, with several deep confidence valleys in between. At earlier times the valleys shrink away, but even at a decade out one could take a hit of as much as 5% to success probability by timing the intercept incorrectly. Also note the 'last chance' window near 3.5 years out that, while no longer certain, has a better than even chance of success.

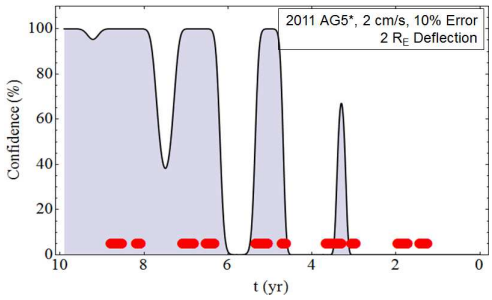

Figure 3: The percent probability that an object with the orbital parameters of 2011 AG5, when given a 2 cm/s impulse with 10% error, will be deflected by $2R_E$ or greater, as a function of time-to-impact. The confidence level peaks in response windows centered around the perihelion point of the orbit. The red dots indicate 100 possible intercept trajectories (using NASA's Trajectory Browser**??**) for a deflection mission assuming an impact date of Feb. 4, 2040.

To be a more useful tool one must fold this curve with the launch windows for an intercept mission. At the bottom of Fig. 3 are 100 red dots that were obtained from the flyby dates given by NASA's Trajectory Browser**??** for flybys in the years leading up to the close approach date for 2011 AG5 of Feb. 4, 2040. This simulates a deflection mission for our fictitious 2011 AG5* object. The flyby dates cluster into several groupings, with some being near confidence peaks or plateaus, and some on the edge or in regions of low probability of success. Mapping these flyby dates to their corresponding launch dates one obtains the launch opportunities and corresponding probability of success shown in Fig. 4.

In Fig. 4 one can see that launch dates varying by as little as a week can effect the confidence level by factors of two or three, as different launch velocities will have missions arriving at differing times. Equally notably there are many launch dates that result in deflection attempts that will be almost completely unable to succeed. These results exemplify the highly nonlinear nature of the underlying orbital problem and propagation of uncertainty through the orbital motion, as well as the nontrivial coupling of launch dynamics with deflection dynamics. Most notably perhaps is the exceedingly narrow launch window for attempts that occur during the 'last chance' peak. All of these launches must occur on the same day: April 7, 2035.

One can ask the question of what higher (or lower) levels of uncertainty in the deflection velocity will do to the confidence in mission success? In Fig. 5 several different confidence curves are plotted for 2011 AG5*, with velocity errors ranging from 1% to as much as 75%. The confidence level associated with a 1% velocity error (in black) shows the expected behavior of tightly defined plateaus and valleys, as the statistical behavior is perturbatively close to the mean

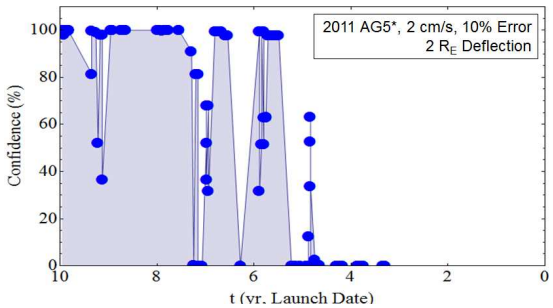

Figure 4: The percent probability that an object with the orbital parameters of 2011 AG5, when given a 2 cm/s impulse with 10% error, will be deflected by $2R_E$ or greater, as a function of launch date (using the NASA Trajectory Browser**??**). This assumes an impact date of Feb. 4, 2040. Note that launch dates varying by as little as a week can cause the confidence level to change by factors of two to three, due to differing flyby dates. Also note that the 'last chance' window launch dates all occur on the same day: April 7, 2035.

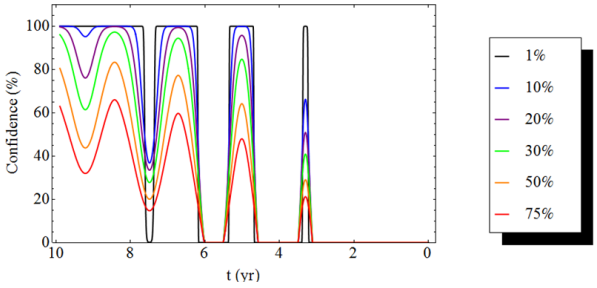

Figure 5: The percent probability that an object with the orbital parameters of 2011 AG5, when given a 2 cm/s impulse with varying error, will be deflected by $2R_E$ or greater, as a function of time-to-impact. As the uncertainty in the deflection velocity increases the overall mission success probability becomes suppressed, especially for the 'last chance' window.

value. The edges of the high-confidence plateaus become blurred as one moves to larger and larger deflection velocity uncertainties, along with an overall suppression of the mission success confidence. This last effect is most significant in the 'last chance' plateau, where at the greatest uncertainty level even a perfectly timed deflection will only succeed one-fifth of the time.

4. Confidence with Differing Orbital Parameters

For an object with different orbital parameters the confidence function will change. Holding one of either the eccentricity or the semi-major axis of 2011 AG5* fixed and changing the other parameter will produce the contour plots in Fig. 6. In Fig. 6(a) the eccentricity is changed while holding the semi-major axis fixed at $a = 1.43$, while in Fig. 6(b) the eccentricity is fixed at $e = 0.39$ and the semi-major axis is changed, resulting in the figures shown. Here, a darker blue region has a higher confidence level, while a white region has a confidence level near zero.

From the plot with changing eccentricity one can see that as the eccentricity increases the response windows narrow a small amount, and the shallow valley at 9.5 years becomes considerably deeper. This most likely reflects the more difficult prospect of intercepting the object near enough to perihelion to make a serious orbital change. Also, the window for the 'last chance'

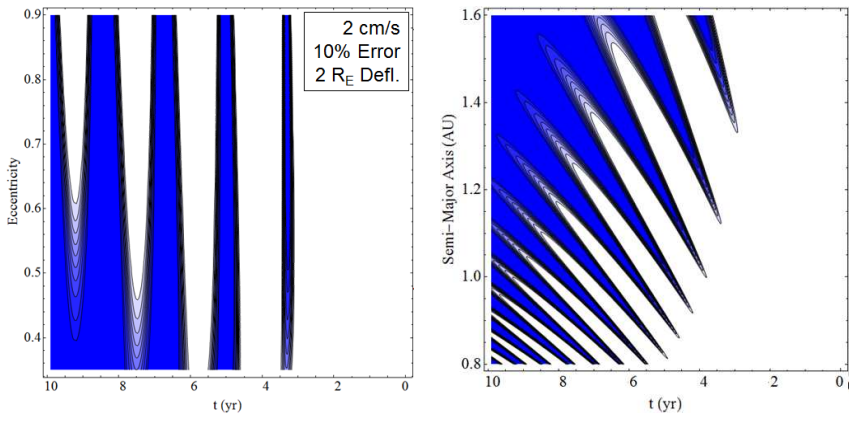

(a) (b)

Figure 6: Contour plots of the confidence level for deflection of 2011 AG5* with mean deflection of cm/s and 10% error, changing eccentricity (a) and semi-major axis (b). Darker blue regions are higher probability. Higher eccentricities seem to have narrower response windows. The shape of the semi-major axis plot is primarily due to the changes to the orbital period as the semi-major axis changes. Higher semi-major axis seem to have fewer, but wider, response windows.

opportunity has a more unique shape due to the special nature of a deflection attempt at that time being a near-run event.

In Fig. 6(b) the overall structure is largely due to the differences in orbital period as the semi-major axis is changed. Note that this gives fewer, but wider, response windows for objects with a large semi-major axis, while for objects with a small semi-major axis there will be many more opportunities but a much narrower window to hit. This raises some interesting conclusions regarding the uncertainties due to the orbital determination of the NEO. While in Fig. 6(a) one can see that small uncertainty in the eccentricity of the object will make only a small difference in the timing of the deflection opportunity, in Fig. 6(b) the changes in window timing come more frequently and occur rapidly as one changes semi-major axis. This is especially true for object will small semi-major axes. Thus it is of vital importance that the semi-major axis of the object be known correctly prior to a deflection attempt, as significant changes in timing may be necessary.

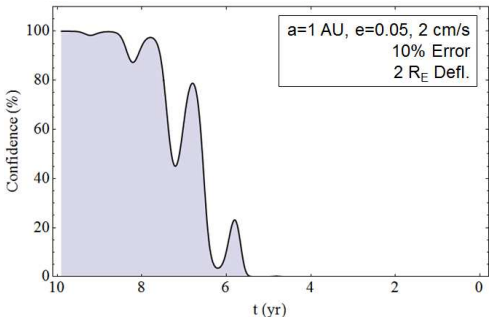

Figure 7: The percent probability that an object with earth-like orbital parameters, when given a 2 cm/s impulse with 10% error, will be deflected by $2R_E$ or greater, as a function of time-to-impact.

In Fig. 7 one can examine the confidence function for an object with orbital parameters that put it on a very earthlike orbit of $a = 1$ and $e = 0.05$. Again, the deflection occurs with 2 cm/s and a 10% error, and we are looking at the probability the deflection will be two earth radii or larger. Here the windows blend together more, with shallower valleys. However, in order to have any chance of a successful deflection the attempt must be made even earlier than in the case of 2011 AG5*, as the 'last chance' window occurs over five years prior to impact.

5. Conclusion

In conclusion, the uncertainties surrounding an NEO deflection attempt spring from many sources. These include object composition, the efficiency of the coupling of the deflection attempt to the NEO, and the original orbital parameters of the NEO. By examining the propagation of errors through the deflected orbit of a fictitious earth-crossing 2011 AG5*, we can pick out several interesting features. While high success probability windows form around orbit perihelion, a greater uncertainty in Δv will broaden these windows slightly but make a significant adverse impact to the success probability. Higher eccentricity objects have narrower response windows, but this changes slowly with changing eccentricity, leading to only a light sensitivity to the accuracy to which the original eccentricity is known. In contrast, the structure of the semi-major axis sensitivity is determined largely by the changes to the orbital period, giving fewer (but broader) windows at high semi-major axis. Furthermore, the timing of the windows is very sensitive to the accuracy of the determination of the NEOs semi-major axis, making this a large possible source of deflection uncertainty. Finally, for an earthlike orbit we found shallower valleys between response windows (making for more forgiving timing), but a much earlier drop to zero confidence, requiring detection and deflection of such an object to occur further out from impact.

[1] Murray, C. D. & Dermott, S. F., Solar System Dynamics, Cambridge, UK: Cambridge Univ. Press, 2000.
[2] Burns, J. A., Elementary derivation of the perturbation equations of celestial mechanics, Am. J. of Phys., 44 (1976), 944.
[3] NASA, http://trajbrowser.arc.nasa.gov/index.php, March 11, 2013.